R-13-51

Flow and transport in fractures in concrete walls in BMA – Problem formulation and scoping calculations

Ivars Neretnieks, Chemima AB

Luis Moreno, LMQuimica

December 2013

Svensk Kärnbränslehantering AB
Swedish Nuclear Fuel
and Waste Management Co

Box 250, SE-101 24 Stockholm
Phone +46 8 459 84 00

ISSN 1402-3091
SKB R-13-51
ID 1416886

Flow and transport in fractures in concrete walls in BMA – Problem formulation and scoping calculations

Ivars Neretnieks, Chemima AB

Luis Moreno, LMQuimica

December 2013

Summary

The walls and bottom plate in the BMA vault in the SFR repository for low and intermediate radioactive waste have been found to have fractures extending through the walls with apertures up to 1.8 mm. Some of the water flowing through the tunnel with the vault may flow through the fractured walls of the vault and carry with it radionuclides from the waste emplaced in the vault. The vault can be surrounded by backfill consisting of crushed rock with large particle sizes that will act as a hydraulic cage allowing only a small fraction of the total flowrate through the tunnel to pass the vault. Nevertheless, the large fractures in the walls will allow water to flow through the waste and carry considerable amounts of nuclides with it. If the large fractures are not sealed the nuclide flowrate can be many orders of magnitude larger than what intact walls would allow. Even if very permeable backfill is used the model simulations suggest that fractures down to a few tenths of a millimeter aperture should be sealed in order not to allow the nuclide transport to become larger than that which will occur by molecular diffusion through unfractured walls. The results apply for sorbing as well as non-sorbing nuclides.

Sammanfattning

Väggarna och bottenplattan i BMA-valvet i SFR-förvaret för låg- och medelaktivt radioaktivt avfall har visat sig ha genomgående sprickor i väggarna med sprickvidder upp till 1,8 mm. En del av det vatten som strömmar genom tunneln med valvet kan strömma genom sprickorna i valvet och bära med sig radionuklider från avfallet inne i valvet. Valvet kan vara omgivet av återfyllning bestående av krossat berg med stora partiklar som kommer att fungera som en hydraulisk bur. Detta tillåter endast en liten bråkdel av det totala flödet i tunneln att passera valvet. Trots detta kan stora sprickor i väggarna tillåta vatten att strömma genom avfallet och bära med sig avsevärda mängder nuklider. Om de stora sprickorna inte täpps kan nuklidtransporten bli många storleksordningar större än vad intakta väggar skulle tillåta. Även om mycket konduktiv återfyllning används tyder modellsimuleringarna på att sprickor med en öppning ner till några få tiondels millimeter bör tätas för att inte tillåta nuklidtransporten att bli större än den som kommer att ske genom molekylär diffusion genom intakta väggar. Detta gäller för sorberande såväl som för icke-sorberande nuklider.

Contents

1 Conceptual picture of the situation and problem posed

1.1 The setting and problem formulation

In the BMA vault the waste is emplaced between vertical concrete walls standing on a bottom plate and overlain by other plates (the lid). This concrete structure is surrounded on all sides, including the bottom, by very permeable sand, gravel or crushed rock acting as a hydraulic cage. If the concrete has very low hydraulic conductivity water that flows through the tunnel, after it has been water filled, will flow essentially only around the concrete structure and very little through the walls of the vault itself. If the concrete develops fractures, some of the water flowing through the tunnel can flow through the walls and thus also through the waste. This water will carry radionuclides when it leaves the vault.

The nuclides in the waste are assumed to be readily accessible to the water seeping through the vault. The waste in the vault can be thought of as well mixed homogeneous mass, everywhere in contact with the seeping water. The non-sorbing nuclides are assumed to be dissolved in the water, whereas the sorbing nuclides are partitioned between water and solid.

The contaminated water leaving the vault through the fractures will be in contact with the fracture surfaces. The nuclides may diffuse from the fracture surface into the unfractured porous concrete and the sorbing nuclides may find sorption sites in the concrete matrix on which to sorb. This can delay the out transport of nuclides from the water inside the vault to the water outside the concrete vault. However, the nuclides also diffuse through the different concrete barriers.

The main question is

- When does fracturing noticeably start to impact the rate of release of nuclides to the water seeping in the rock compared to when the concrete is so little fractured that it can be treated as a homogeneous medium through which the nuclides escape only by molecular diffusion?

This question can be broken down into operative questions

- At what rate are nuclides released from an un-fractured vault to the water seeping in the surrounding rock?
- How much water will flow through the vault and waste?
- How much nuclides will be carried by the water that flows through fractures in the concrete and leaves the tunnel?

1.2 Approach

In order to highlight the important mechanisms and processes we simplify the geometry of the tunnel and the hydraulic setting as shown in Figure 1-1. Table 1-1 summarises the dimensions of the constructions and Table 1-2 gives some hydraulic data. Table 1- 3 summarises diffusion and other transport properties of concrete.

These data will be used for illustrative modelling and to obtain first impressions of how fractures can impact the release of the nuclides. These results will also show the sensitivity of the results to the various entities and point to where the uncertainties are largest.

1.3 Data

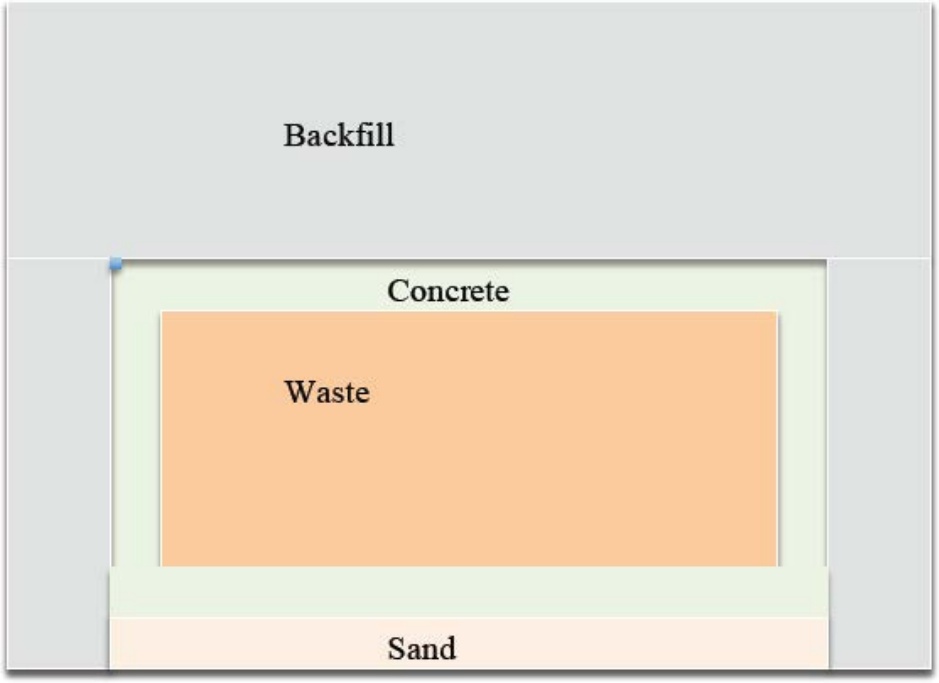

Figure 1-1. *Cross section of idealised drift and vault after Figure 9.5 in Holmén and Stigsson (2001).*

Table 1-1. Summary of the dimensions of the different parts, from Holmén and Stigsson (2001, Figure 9.6) (called HS).

Notation	Meaning	Value	Reference or comment
L_T	Length of tunnel	160 m	HS
L_V	Length of concrete vault	133 m	HS
W_T	Width of tunnel	20 m	HS
W_V	Width of vault	16 m	HS
H_T	Height of tunnel	16 m	HS
H_V	Height of vault	8 m	HS
d_{Con}	Thickness of concrete	0.4 m	Vertical and horizontal taken the same[1] HS
d_B	Vertical backfill filling thickness	2 m	HS
H_{BT}	Thickness backfill on top	6 m	HS
H_{SB}	Thickness of sand at bottom	1 m	HS
A_V	Cross section area of vault $L_V \times H_V$	1064 m^2	
A_{SB}	Cross section area sand in bottom $L_V \times H_{SB}$	133 m^2	
A_{ST}	Cross section area backfill on top and on sides of tunnel $L_T \times H_T - A_V - A_{SB}$	1363 m^2	

[1] The thicknesses is simplified to be the same as it has marginal consequences for the subsequent modelling.

Table 1-2. Summary of hydraulic and related properties of the different materials.

K_S	Conductivity of sand	10^{-5} m/s	HS
K_B	Conductivity of backfill	[2]	Equation (2–9)
K_{Con}	Conductivity of structural concrete	8.3×10^{-10} m/s	SKB (2014)
T_{Cub}	Transmissivity of fractures according to cubic law		Equation (2–5)
k_T	Decrease factor for transmissivity due to constrictions	0.1, 0.3 and 1	For illustration
δ	Examples of fracture aperture	0.1, 0.3 and 1 mm	SKBdoc 1430853, Akhavan et al. (2012)
P_{21}	Fracture density, m/m^2	0.25 /m	SKBdoc 1430853

Table 1-3. Summary of other properties of the different materials.

ρ_{Bulk}	Bulk density of concrete	2530 kg/m^3	SKB (2014)
D_W	Diffusion coefficient in water	2×10^{-9} m^2/s	Same as above
D_{SC}	Diffusion coefficient in structural concrete (Effective)	3×10^{-12} m^2/s	Same as above
D_{BS}	Diffusion coefficient in backfill and sand (Effective)	6×10^{-10} m^2/s	Same as above
ε_{SC}	Porosity of structural concrete	0.15	Same as above
ε_{BS}	Porosity of backfill and sand	0.3	Same as above
Q_{tot}	Total flowrate through the BMA tunnel	50 m^3/yr.	Example from Holmén and Stigsson (2001)[3]

[2] Estimates of the hydraulic conductivity of backfill are made for which the conductivity is expected to be considerably higher than for sand. This will impact the flowrates through the fractures.

[3] When the repository is below the sea the flowrate is very low. After land-rise it increases to 50 m^3/yr at 3000 AD. At this time the travel time from repository to the biosphere is the shortest.

2 Modelling flowrates through walls in vault and waste

In this chapter a simple model is developed which allows the flowrate through the fractured walls of the vault to be estimated. Several simplifying assumptions are made. A commonly used relation for the hydraulic transmissivity of fractures is presented as well as a relation for the hydraulic conductivity of a bed of particles. The idealised theoretically derived relation for fracture transmissivity must be supplemented by an empirically derived correction factor, which can vary widely. The likewise theoretically derived relation for the hydraulic conductivity of a porous bed is less uncertain but also there some empiricism is involved. Although there are uncertainties the relations are deemed to be sufficiently accurate for the purpose of the present report.

2.1 Flow model as resistance network

The water flowrates in the different parts of the BMA repository can be estimated by using a simple flow conductance network model. It is analogous to an electrical conductance model. Figure 2-1 shows such a model applied to the conditions in BMA. It will later in the examples be assumed that the flow is horizontal and perpendicular to the tunnel.

Figure 2-1 show a network of flowpaths with flowrates and conductances. C is the conductance and Q the flow rate. Subscripts "*Up*" means that the flow is through the backfill above the concrete vault, "*Concrete*" that is the flow through the fractured concrete and "*Low*" that the flow goes through the sand below the vault.

The low conductivity of the rock determines the overall flowrate Q_{tot} through the vault because the other conductances are very much higher.

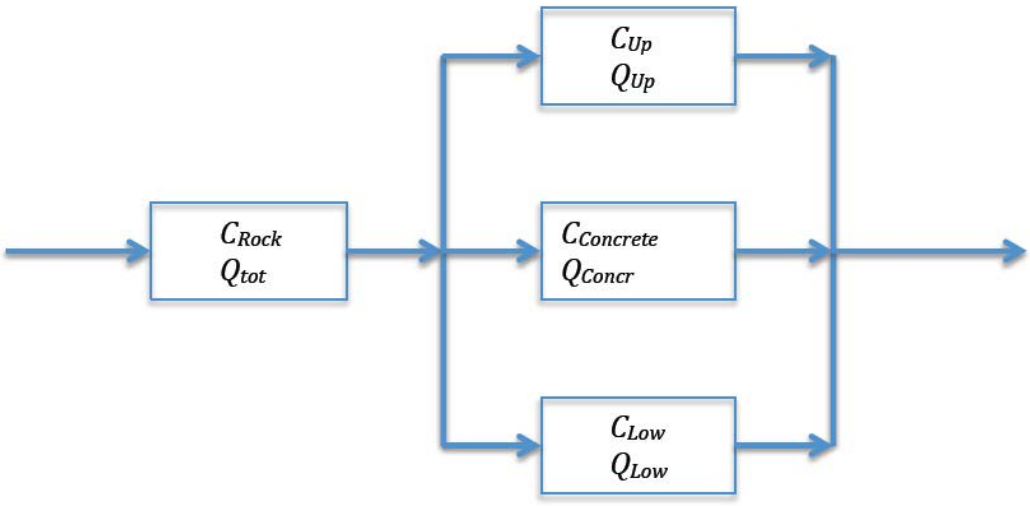

Figure 2-1. *Simplified picture of the flowpaths in BMA.*

The flowrate in each path is determined by Darcy's law for one-dimensional flow.

$$Q_j = K_j A_j (h_1 - h_2)/d_j = C_j (h_1 - h_2) \quad (2\text{-}1)$$

h_1 and h_2 are the hydraulic heads at the rock interfaces, K_j the hydraulic conductivity, A_j the cross section for flow of each medium, and d_j the thickness in the flow direction. To shorten the notation we use the notation C for conductance

$$C_j = K_j A_j / d_j \quad (2\text{-}2)$$

For these conditions, when the conductivity of the rock is very much lower than either that of sand or backfill, the rock conductivity and the hydraulic gradient in the rock determines the total flowrate Q_{tot} passing the tunnel. For these conditions Q_{tot} is practically independent of the construction of the vault.

The flowrate in each medium in the tunnel, *j,* then becomes

$$Q_j = \frac{Q_{tot} C_j}{\Sigma C_j} \quad (2\text{-}3)$$

It is seen that, given the properties and geometry of concrete, sand, and backfill, the flowrate through the concrete is essentially directly proportional to its conductivity because the sand and the backfill are chosen such that it has a very high conductivity and $C_{Concrete} \ll C_{Low}$ and C_{Up}.

$$Q_{Concrete} \cong \frac{Q_{tot} C_{Concrete}}{C_{Low} + C_{Up}} \quad (2\text{-}4)$$

Choosing a backfill with a very high conductivity will minimise the flow through the concrete even if it is fractured. Methods to estimate hydraulic properties of fractures and porous media are treated next.

2.1.1 Transmissivity of individual fractures

For flow in a slit with smooth walls the transmissivity is given by the cubic law (Bird et al. 2002, p 63)

$$T_{Cub} = \frac{\varrho_w g}{12 \eta_w} \delta^3 \quad (2\text{-}5)$$

δ is the fracture aperture, ϱ_w is the density of water, g is the gravitation constant and η_w is the viscosity of water.

$T_{Cub} \cong 8 \times 10^5 \delta^3$ m^2/s for water at ambient temperature if the aperture is given in m.

Real fractures can have much smaller transmissivities because their aperture varies and can contain constrictions. For the real fracture we introduce a correction factor k_T, smaller than 1 and typically in the range 0.1-1. The transmissivity for a real fracture becomes

$$T_{Real} = k_T T_{Cub} \quad (2\text{-}6)$$

It is expected that fractures with large apertures, especially when fracture surfaces are not much in contact, will have k_T near one, whereas narrow fractures will have smaller values of k_T.

2.1.2 Conductivity of a fractured medium

The concrete wall is envisaged as having a number of fractures that intersect it with some angle to the normal. For simplicity it is assumed that they are perpendicular to the wall. The length of the fractures is equal to the wall thickness. The density of the fractures is described by the total trace length of fractures per wall area, P_{21} [m/m^2]. P_{21} can also be seen as the inverse of the mean distance, S, between fractures if they were parallel. If all fractures have the same transmissivity and the water flows only through the fractures, the hydraulic conductivity of the wall is

$$K = T_{Real} P_{21} = T_{Cub} k_T P_{21} \quad (2\text{-}7)$$

Equation (2-7) will be used to calculate the mean conductance of the fractured concrete vault.

2.1.3 Hydraulic conductivity of a porous bed of particles

A simple and commonly used model to estimate the hydraulic conductivity of a bed of particles is given by the Kozeny-Carman equation (Coulson and Richardson 1991, p 136).

The flowrate Q for an area A of bed is obtained from

$$Q = KA\frac{dh}{dx} \tag{2-8}$$

$\frac{dh}{dx}$ is the hydraulic gradient. The hydraulic conductivity K of a porous bed consisting of spherical particles with diameter d_p and porosity ε_B is

$$K = \frac{d_p^2}{180}\frac{\varepsilon_B^3}{(1-\varepsilon_B)^2}\frac{\varrho_w g}{\eta_w} \tag{2-9}$$

The constant 180 is also cited to be 150 in another well-known book (Bird et al. 2002, p 191). In Green and Perry (2008, pp 6–39) a value of 200 is given. The differences are partly due to different assumptions on how the tortuosity is handled. For non-spherical particles the particle diameter d_p is idealised and is taken equal to that of a sphere with the same volume as the particle. Real particles can have uneven shapes and edges, which makes the surface larger than that of a spherical particle. A shape factor φ_s can be used to account for this. The shape factor $\varphi_s < 1$ shows how much smaller a sphere must be to have the same surface to volume ratio as the real particle. In addition, when there is distribution of particle sizes this is accounted for by a weighting procedure that gives the mean surface area per volume of particles. This is given by

$$\frac{1}{d_{p,mean}} = \sum_i \frac{x_i}{d_{p,i}} \tag{2-10}$$

x_i is the mass fraction of particles with diameter $d_{p,i}$. Introducing this and the shape factor in Equation (2-9) gives

$$K = \frac{\varphi_s^2 d_{p,mean}^2}{180}\frac{\varepsilon_B^3}{(1-\varepsilon_B)^2}\frac{\varrho_w g}{\eta_w} \tag{2-11}$$

The expression has been fairly well verified by experiments for spherical particles of equal size and for a variety other shapes and mixtures of particle sizes although the constant, 180 in this example varies somewhat.

Equation (2-11) will be used to calculate the mean conductance of the backfill and the sand to obtain the flowrate through the vault. This flowrate will carry with it the nuclides in the waste inside the vault. The transport by flow will be compared with the transport through the walls, bottom and lid by molecular diffusion. The latter is discussed next.

3 Transport by diffusion through the concrete walls

In this model it is assumed that once the rock vault and concrete structure have become water filled, the nuclides in the waste have been dissolved in the pore water in the waste. Sorbing nuclides will partition between the water and solids in the waste. The nuclides start to diffuse into the containing walls of the vault. It takes time for them to penetrate to the water in the porous backfill and sand that surrounds the vault. The rate of transport to the outside of the walls increases and reaches a steady state transport rate if the concentration inside the waste does not decrease much.

The governing equation that describes this process is

$$R_p \frac{\partial c}{\partial t} = D_p \frac{\partial^2 c}{\partial x^2} \text{ or} \tag{3-1}$$

$$\frac{\partial c}{\partial t} = D_a \frac{\partial^2 c}{\partial x^2} \tag{3-2}$$

where

$$D_a = D_p/R_p \tag{3-3}$$

is the apparent diffusivity

R_p is the retardation factor of the nuclide.

$$R_p = 1 + \frac{K_d \rho_{Bulk}}{\varepsilon_{Con}} \tag{3-4}$$

ρ_{Bulk} is the mean density of the minerals in the concrete.

The initial and boundary conditions needed to solve the equation are

$c = 0$ at $t = 0$ for all x (3-5)

$c = c_o$ at $x = 0$ for all t and (3-6)

$c = 0$ at $x = d_{Con}$ for all t (3-7)

The latter condition assumes that the nuclide is rapidly diluted in the large volume of water flowing in the backfill and sand. The solution for the evolution in time and space is (Carslaw and Jaeger 1959, p 310)

$$\frac{c(t,x)}{c_o} = \sum_0^\infty (Erfc[\frac{(2n+1)d_{Con} - (d_{Con} - x)}{2\sqrt{D_a t}}] - Erfc[\frac{(2n+1)d_{Con} + (d_{Con} - x)}{2\sqrt{D_a t}}]) \tag{3-8}$$

Figure 3-1 below shows the concentration evolution in the concrete wall for base case data for non-sorbing nuclides. After 30 to 100 years the transport has approached and practically reached steady state. For sorbing nuclides with a retardation factor R_p the time will increase with the retardation factor. For a nuclide with a retardation factor equal to one hundred it will take 3000 to 10,000 years for steady state to be reached.

The time to reach steady state for diffusion can also be roughly estimated by

$$t_{SS} = \frac{d_{Con}^2}{2\, D_a} \tag{3-9}$$

This gives a value of 127 years for the case above.

The diffusion through the walls will start shortly after the concrete in the vault and the waste are water filled. Flow through the walls will effectively start after land-rise has increased the hydraulic gradient considerably.

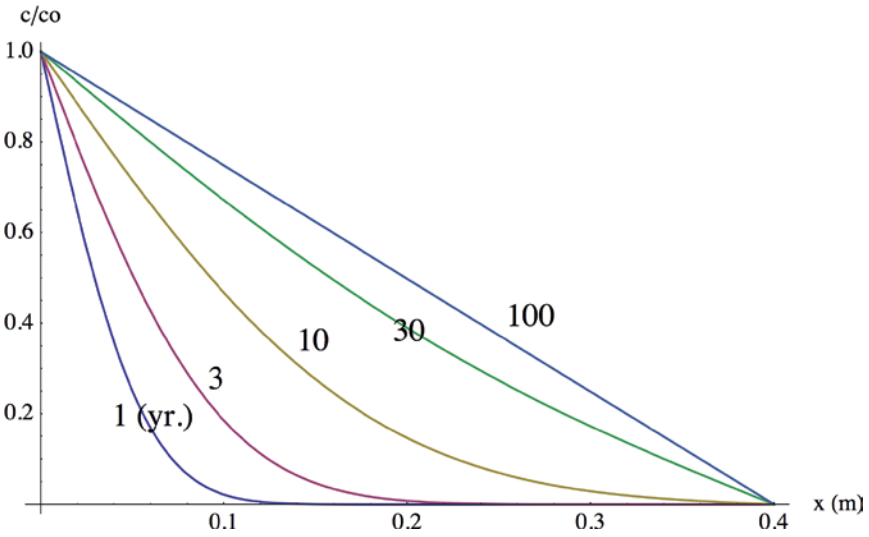

Figure 3-1. *Concentration evolution in the concrete wall for base case data.*

4 Comparison of transport by flow in fractures and by diffusion through walls

For steady state transport by diffusion the flowrate of a nuclide N_D from the entire vault is

$$N_D = D_e A \frac{c_o}{d_{Con}} \quad (4\text{-}1)$$

A here is the sum of the areas of the walls, bottom and lid. Here it is assumed that the nuclide at the outside is rapidly diluted in the water in the backfill and has a negligible concentration compared to c_o. For steady state transport in fractures by flow the rate of transport N_Q is

$$N_{Q\_} Q_{Con} c_o \quad (4\text{-}2)$$

For the transport by flow the time to reach the outside is longer than the water residence time in the fractures in the concrete wall because the nuclides are retarded by matrix diffusion. This is discussed in the next chapter.

The ratio of transport by flow to that by diffusion is N_Q/N_D and will be used later to illustrate what fracture aperture and frequency as well as particle sizes in the backfill could lead to release rates by flow that are larger than those by molecular diffusion through the intact concrete walls.

5 Transport of nuclides through a fracture

For many sorbing and decaying nuclides steady state conditions may never be reached. Also the water residence time in the fractures does not say when the nuclide from the inside starts to flow out at the exit of the fracture. It can come much later. The concentration of the nuclide over time at the exit of the fracture, i.e. as it has passed the concrete wall is modelled below. It will be used later to assess if the retardation in the fracture can help to decrease the rate of transport by flow. In chapter 4 it was assumed that the flowing water carried with it the nuclide in the same concentration as in the waste.

When water with solutes flows in a fracture in a porous medium, such as concrete, the solute will diffuse in and out of the pores in the concrete matrix. Non-sorbing nuclides will gain access to a larger water volume than that in the fracture and thus will have a longer residence time that that of the flowing water. Sorbing nuclides will in addition sorb on the inner surfaces of the concrete and be additionally retarded. A sorbing nuclide with an initial concentration c_o, decaying with a decay constant l, that is fed into the fracture will emerge at the outlet with a concentration that varies in time. Neglecting any hydrodynamic dispersion in the fracture the effluent concentration is (Neretnieks 1980)

$$c(t) = c_o e^{-\lambda t} Erfc(\frac{FWS}{Q}\frac{MPG}{\sqrt{t-t_o}}) \quad (5\text{-}1)$$

FWS is the flow-wetted surface of the fracture that the flowrate Q contacts. It may be noted that the entity $\frac{FWS}{Q}$ also played a central role for the modelling of the friction when determining the hydraulic properties of the fractures and the backfill. *MPG* is a materials property group that accounts for the access of the pore volume and inner surfaces of the concrete on which the sorbing nuclide can attach itself. t_o is the water residence time. The equation is valid for times longer than the water residence time.

$$MPG = \varepsilon_{Con}\sqrt{D_p R_p} \quad (5\text{-}2)$$

ε_{Con} is the porosity of concrete, D_p is the pore diffusion coefficient.

Equation (5-1) can be used to estimate when the nuclide begins to exit the fracture. To illustrate this an entity called "early breakthrough time" $t_{0.001}$ for a stable nuclide can be defined. This is the time when the concentration at the outlet has reached 0.001 c_o. It is obtained by solving Equation (5-1) for the time when c/c_o. = 0.001. This will be used later in the examples assuming no decay.

It should be noted that Equation (5-1) is valid only when there is only diffusion in the direction perpendicular to the fracture and not in same direction as the fracture. Such conditions apply with a fair approximation for fractures that are long compared to the diffusion depth into the concrete matrix. That is not the case here because, as was shown in chapter 3, a non-sorbing nuclide will attain a steady state concentration profile through the concrete after about 100 years. The nuclide carried by the flowing water in the fracture will not have an un-contaminated or little contaminated concrete into which it can diffuse, at least not in the first part of the fracture. Equation (5-1) exaggerates the delay by diffusion. However, it can be used for qualitative estimates. For large $t_{0.001,}$ if the term $\frac{FWS}{Q}$ *MPG* is much larger than $\sqrt{t_{0.001} - t_o}$ even a small part of the FWS i.e. the later part of the fracture where to concentration in the matrix is lower than c_o will act as a strong sink for the nuclide carried by the water in the fracture. The entity $t_{0.001}$ if much larger than t_{ss} will therefore at least qualitatively indicate that the effluent concentration can be expected to be much lower than c_o and that the steady state N_Q derived by Equation (4-2) can be considerably exaggerated.

It is possible to do more accurate simulations of N_Q using numerical solutions of the equations that describe the two-dimensional transport of solutes in a medium intersected by thin fractures with flowing water. However, the numerical solutions, especially with very thin fractures, are not always straightforward and accurate. We will do these calculations in a later version of this report, if necessary.

6 Fracture apertures and frequency

In this chapter the frequency of fractures and their apertures observed in BMA are presented. Observations and experiments to determine fracture transmissivities in concrete are presented and discussed as well as how and why fractures form in concrete. Some observations of self-healing of fractures in young concrete are mentioned as well as how self-sealing could be promoted.

6.1 Fractures in BMA

Hejll et al. (SKBdoc 1430853) inspected a 40 m long empty section of the BMA tunnel. They observed fractures in the bottom floor and vertical walls and measured fracture apertures. Most of the fractures extended through the walls, which could be observed from inside as well as from the outside of the walls. Some of the fractures were located at the pouring joints but there were also fracture in the walls between the joints. In total apertures of 14 fractures in the vault walls and 13 apertures in the floor were reported. There were additional fractures where the apertures were not reported. In total 21 fractures were shown on the maps of the walls. Practically all of the nearly vertical fractures are seen on both sides of the walls. In the floor the fractures could only be seen from one side for obvious reasons. The apertures ranged from 0.1 to 1.8 mm. 8 of them have apertures between 1.5 and 1.8 mm. Not all fractures extended over the entire height of the wall. All the fractures are deemed to be caused by shrinking contraction of the concrete as it cools after the pouring when it is warmed by the chemical reactions during the settling.

A rough measure of the mean distances, S, between the fractures in the walls and the floor are then 80/21 = 4 m and 40/13 = 3.1 m respectively.

6.2 Fracture transmissivities in concrete

There are only few experimental studies of transmissivities in fractures in concrete. Akhavan et al. (2012) presents a short review of some earlier studies. They also performed a number of measurements of the transmissivity of fractures induced in cylindrical cores in month old cured cement. The apertures measured by the measured expansion of the core, the so called COD (Crack Opening Displacement) ranged up to about 0.2 mm. Similar aperture values were obtained by digital scanning of the opened fractures. Transmissivities were measured by injecting water at a known over pressure and measuring the flowrate during 15 minutes. During longer test times the transmissivity decreased gradually. It was found the transmissivity decreased by up to 85% over a period of 24 hours. Similar decreases of transmissivities in similar aperture fractures were also observed by Aldea et al. (1999) and by Li et al. (2011). The Akhavan et al. (2012) transmissivities qualitatively followed the cubic law (Equation 2-5) but were about a factor of 5 –6 lowerr, $k_T = 0.2$. Picandet et al. (2009) also found qualitative agreement with the cubic law on fractures apertures up 0.4 mm. Narrower fracture apertures seem to deviate more from the cubic law than larger. The largest apertures reported in the above investigations were 0.4 mm.

It is speculated by the authors of the present report that the rather narrow fractures used in the above cited investigations may be more influenced by fracture roughness and flowpath tortuosity than larger aperture fractures such as the more than 1 mm fractures in BMA. In the later sample calculations it is therefore assumed that the cubic law is valid for the larger fractures, whereas the transmissivity in fractures with tenth(s) of millimetre apertures may have lower transmissivities than what cubic law predicts.

6.3 Fracture formation in concrete

Hejll et al. (SKBdoc 1430853) give a short description of fracture formation in concrete caused by the shrinking of the concrete as it cools after pouring and initial hardening. During the hardening, as the various components in the cement take up water and form new compounds, heat evolves and increases the temperature by several tens of degrees. When the reactions near completion and slow down the concrete slowly cools down. In thick constructions the cooling takes longer time than in thin. In thick constructions the cooling near the surface is faster than further inside the construction. As the concrete cools it shrinks. If the construction as a whole cannot shrink evenly, fractures form. The shrinking is typically on the order of a fraction of one mm per metre or more. This leads to the observed fracture apertures of more than one mm in BMA. Fractures are also formed in concrete constructions by uneven mechanical loads. Thin hairline fractures are also observed in concrete constructions. It is outside the scope of the present report to discuss the formation mechanisms in more depth. We will assess the consequences of the presence of fractures of different sizes on the radionuclide release in order to see what fracture sizes and frequencies will not significantly increase transport and what sizes and frequencies will.

6.4 Damages caused by corroding iron reinforcements

There is a large number of steel bolts that extend through the walls of the BMA. They have a mean spacing of about 1 m. When the bolts corrode the corrosion products expand and generate tensile stresses in the walls. It is conceivable that fractures can be induced between the bolts. Such fractures do not seem to have been observed in BMA, Nevertheless, we explore a “what if “case by assuming that numerous such tensile fractures form. The corroded bolts themselves are assumed to be hydraulically tight.

6.5 Healing of fractures in concrete

There are several observations and experimental studies of self-healing of fractures in concrete. Typically in the experiments a cylindrical core with the fracture is sealed on the sides so that water can be injected at one end and collected at the other end. The flowrate is measured for a known pressure difference. Transmissivity of the fracture is obtained from these data and from the length and width of the core. Fracture apertures between 0.1 an 0.4 mm have been tested in different experiments with different cements. In the experiments it was found that the transmissivity of the fracture dropped quickly initially and slowed down after weeks to months. Typically decreases of a factor of 7-10 and sometimes more were observed after month or months. Some specific investigations are mentioned below.

Gagné and Argouges (2012) found that small (50 μm) cracks generated in one and six month old mortars self-sealed at rates of 10–20 μm/month when subjected to air at 100% relative humidity. Larger cracks (200 μm) sealed 15–30 μm/month whereas 300 μm sealed slower, 20% over five months. The sealing was caused by precipitation of calcite. Akhavan et al. (2012) found that the fracture transmissivity decreased up to 85% in 24 hours in recently formed fractures (10 to 200 μm) subject to water flow. Both calcite formation and hydration of as yet un-hydrated cement caused this effect. Similar findings are reported by Aldea et al. (1999) and Li et al. (2011).

Two main reasons for the closing of fractures are cited. One is that some cement particles have not hydrated fully before the start of the experiment and that when water is injected into the fracture, the as yet un-hydrated cement hydrates and swells to close the thin fracture. The other main mechanism cited is that carbonate that intrudes the fracture precipitates with calcium released from the portlandite and forms calcite, which precipitates in the fracture. Investigations of self-sealing of larger than 0.4 mm fractures have not been found in the literature.

There is a number of recent papers on how self-sealing and self-repairing concrete can be formulated. A list of references is available the Appendix. Some of the proposed methods are based on adding an organic compound that together with some special, also added microorganisms, will produce carbon dioxide by microbially mediated oxidation of the organic compound. The carbon dioxide will

precipitate as calcite and seal the damages. There is experimental evidence that such self-healing occurs. This is not further discussed in the present report because the BMA vault is constructed already. It may be something to consider for coming underground constructions, though.

In none of the investigations cited above any modelling of these processes based on the chemical reactions, the reaction rates and transport of the reacting species are presented. At present it is not possible, based on the above observations, to make any credible predictions of the rates of fracture sealing that may happen in the BMA repository.

7 Sample calculations

Sample calculations are presented based on the base case data in chapter 1 and for different combinations of fracture apertures and frequencies and sizes of backfill particles.

Different fracture apertures are used. One is based on the observed fractures in BMA described in chapter 6. In the examples an aperture of 1 mm is used combined with a k_T of 1. This combination is deemed to be reasonably realistic for the large fractures observed. A fracture frequency P_{21} of 0.25 is used, this is within the range of observed values at BMA. Another set of fracture data is selected to illustrate hypothetical fractures that might be generated by tensile stresses caused by the corroding iron bolts in the walls of BMA. Table 7-1summarises the data and the resulting hydraulic conductivities of the fractured concrete. The conductivity of un-fractured concrete is several orders of magnitude lower than that of even mildly fractured and flow through it will be negligible. It is not further considered.

Table 7-2 summarises the different calculations with combinations of small and large fractures together with different particle sizes of the backfill particles, 0.5, 5 and 50 mm. The size of the backfill particles can be thought of as e.g crushed rock that is sieved to have a narrow range of particle sizes. The smallest particles in the range being 5 or 50 mm respectively and the larger particle in the 7 and 70 mm respectively. A rather narrow range should be used in order ensure that the backfill does not segregate when emplaced. Column 4 gives the hydraulic conductivity for the backfill. Column 5 gives the flowrate through the fractured concrete. In column 6 ratio of nuclide transport by the *flow* through the vault to the transport by *diffusion* through all the walls of the vault is given. The latter is un-avoidable and can be seen as a "normal" release rate. The release ratio N_Q/N_D is given for steady state conditions. It shows how much fracturing in the walls can increase the release rate. The next column gives the water residence time t_o for the water flowing in the fractures in the walls. It shows that except for Cases 3, 6 and 9 the residence time is short compared to the time to reach steady state diffusive transport $t_{ss,}$ which was found to be on the order of 100 years in chapter 3. The last column gives the entity $t_{0.001,}$ which is the time for the concentration at the outlet of the fracture to reach 0.001 $c_{o,}$ provided the distance between fractures is very large. This time was calculated for parallel fractures in the concrete wall. The distance between fractures was 0.5 m for small fractures, and 2 m for 1-mm fractures. When $t_{0.001}$ is less than t_{ss} the rate of transport through the fractures has already started to contribute to the release from the vault. The parenthesis around the long times indicate that they are not valid because diffusion through the wall has already allowed the nuclide to penetrate it.

In practice for non-sorbing nuclides, after about 100 years, the transport will be dominated by diffusion through walls with small fractures. When the fractures are larger transport by flow will dominate and start already before 100 years. Uptake into the concrete from the water flowing in the fractures will in practice have a small overall impact in all cases. Sorbing nuclides will be retarded but when steady state conditions have been reached N_Q/N_D is not influenced. Decay may change the ratio by allowing less time for decay when flow is rapid.

Table 7-1. Hydraulic conductivity of un-fractured and fractured concrete

	δ **aperture [mm]**	P_{21} **[m/m²]**	$S=1/P_{21}$ **[m]**	K **m/s**
Construction concrete (intial state)	–	–	–	8.3×10^{-10}
Small fractures	0.1	1	1	8.2×10^{-8}(k_T= 0.1)
Intermediate fractures	0.3	1	1	6.6×10^{-6}(k_T= 0.3)
Large fractures	1	0.25	4	2.0×10^{-4}(k_T= 1)

Table 7-2. Results for the different cases

CASE	Fracture aperture mm	Backfill, $\varphi_s d_{p,mean}$ [mm]^4	Backfill, K_B [m/s]	Concrete, Q_{Concr} [m^3/y]	N_Q/N_D	t_o [y]	$t_{0.001}$ [y]
1	0.1 (k_T = 0.1)	0.5	0.00075	0.11	71.6	0.40	42.4
2	0.1 (k_T = 0.1)	5	0.075	0.0011	0.71	40	(4.8×10^4)
3	0.1 (k_T = 0.1)	50	7.5	1.1×10^{-5}	0.0072	4000	(5.9×10^6)
4	0.1 (k_T = 1)	0.5	0.00075	1.0	703	0.04	0.46
5	0.1 (k_T = 1)	5	0.075	0.011	7.2	4.0	(2800)
6	0.1 (k_T = 1)	50	7.5	1.1×10^{-4}	0.072	400	(5.6×10^5)
7	0.3 (k_T = 0.3)	0.5	0.00075	7.3	5.0×10^3	0.017	0.025
8	0.3 (k_T = 0.3)	5	0.075	0.086	58	1.5	67
9	0.3 (k_T = 0.3)	50	7.5	8.6×10^{-4}	0.58	150	(6.2×10^4)
10	1 (k_T = 1)	0.5	0.00075	42	2.8×10^4	4×10^{-4}	0.0025
11	1 (k_T = 1)	5	0.075	2.5	1700	0.042	0.047
12	1 (k_T = 1)	50	7.5	0.027	18	4.0	46.2

The examples above suggest that the size of the backfill particles and especially the fracture aperture strongly can influence the release of nuclides through the fractures in the concrete walls. Below, some diagrams are presented that will help to assess when fracturing matters and when not. The diagrams show how N_Q/N_D varies with fracture aperture for different k_T and particle sizes of backfill.

Figures 7-1 to 7-6 show the ratio of nuclide transport by flow through the outflow wall of fractured concrete to that by molecular diffusion through the two walls, bottom, lid and the two short side-walls when steady state conditions are reached for diffusion.

In Figure 7-1, it is seen that if the backfill particle size 50 mm is used and the fracture aperture follows the cubic law, the transport through fractures 0.3 mm wide would contribute as much to release as that by diffusion. It may be noted that in this figure the transmissivity is assumed to follow the cubic law. This is a quite conservative assumption. In Figure 7-2 a correction factor to the cubic law $k_T = 0.1$ is used, which on the other hand may not be entirely conservative. Then fractures of about 0.5 mm would give the same release as that by diffusion. A tentative criterion could be used for comparisons saying that an increase of release by an amount equal to that by diffusion could be tolerated. Fractures with apertures of 1 mm would contribute with 100 times larger release than by diffusion when $k_T = 1$. For large aperture fractures it may be expected that k_T is large and a value of 1 may not be unrealistic in fractures generated by tensile stresses.

Figure 7-3. Shows that for the smaller particle backfill (5 mm) only 0.05 mm fracture apertures can be tolerated. Similarly Figure 7-4 shows that 0.1 mm fractures could be tolerated if the transmissivity is ten times lower than what the cubic law suggests.

Figure 7-5 shows that for the smaller particle backfill (0.5 mm) even with 0.01 mm fracture apertures transport by flow dominates. Similarly Figure 7-6 shows that 0.02 mm fractures could just be tolerated if the transmissivity is ten times lower than what the cubic law suggests.

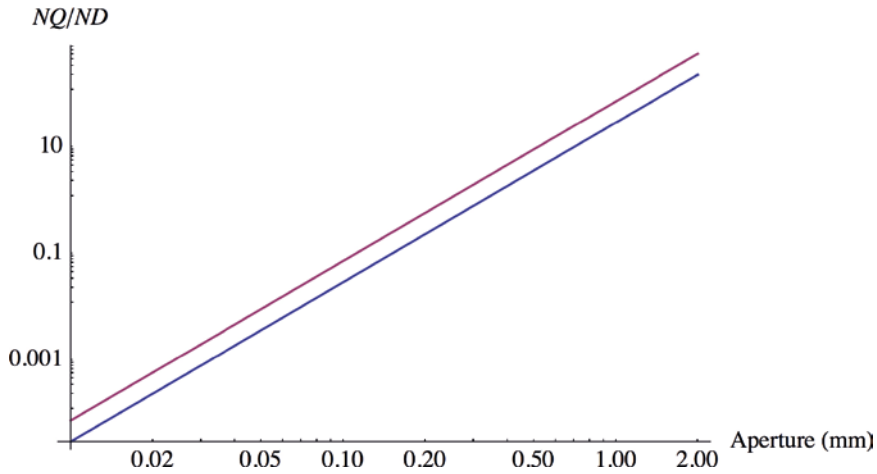

Figure 7-1. *Ratio of nuclide transport by flow to that by diffusion as function of fracture aperture. $k_T = 1$ and $d_p = 50$ mm. Upper curve for $P_{21} = 1$ and lower for $P_{21} = 0.25$ m^{-1}*

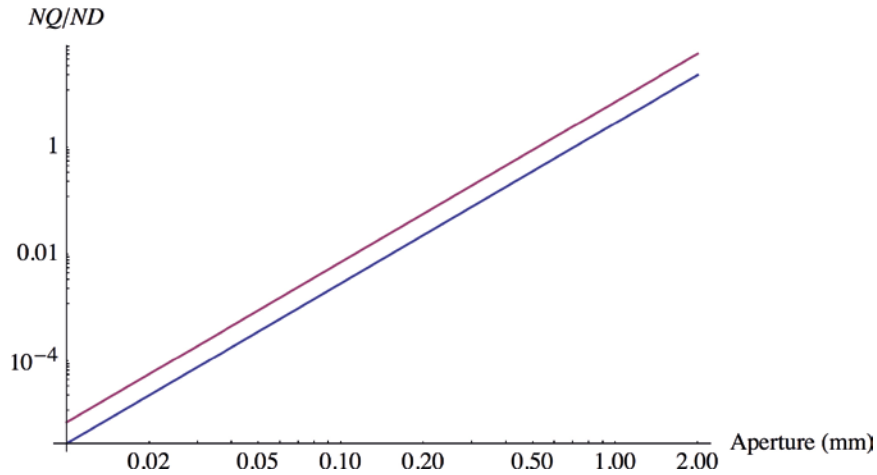

Figure 7-2. *Ratio of nuclide transport by flow to that by diffusion as function of fracture aperture. $k_T = 0.1$ and $d_p = 50$ mm. Upper curve for $P_{21} = 1$ and lower for $P_{21} = 0.25$ m^{-1}*

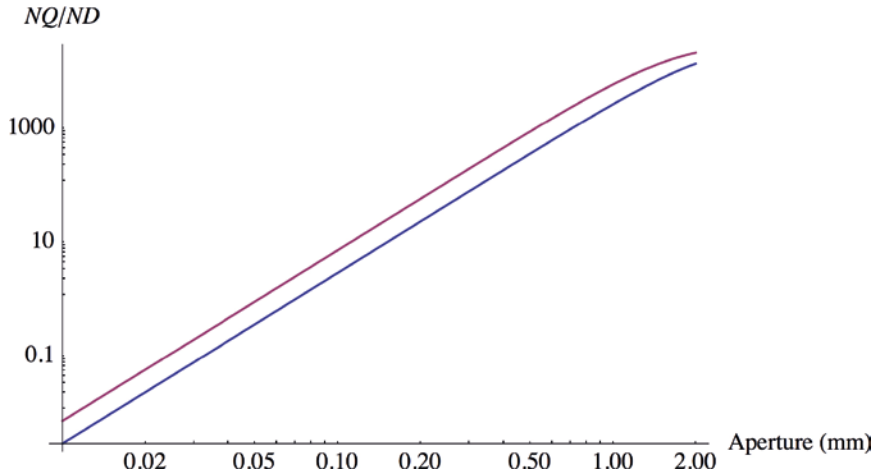

Figure 7-3. *Ratio of nuclide transport by flow to that by diffusion as function of fracture aperture. $k_T = 1$ and $d_p = 5$ mm. Upper curve for $P_{21} = 1$ and lower for $P_{21} = 0.25$ m^{-1}*

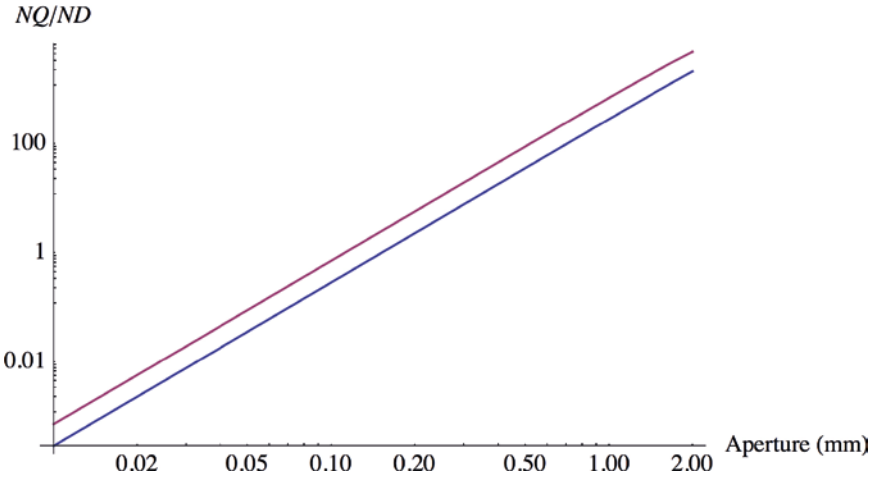

Figure 7-4. *Ratio of nuclide transport by flow to that by diffusion as function of fracture aperture. $k_T = 0.1$ and $d_p = 5$mm. Upper curve for $P_{21} = 1$ and lower for $P_{21} = 0.25$ m^{-1}*

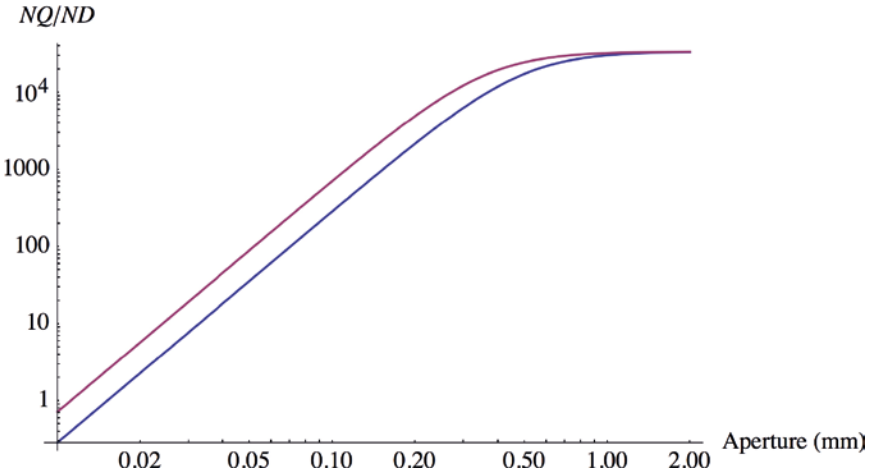

Figure 7-5. *Ratio of nuclide transport by flow to that by diffusion as function of fracture aperture. $k_T = 1$ and $d_p = 0.5$ mm. Upper curve for $P_{21} = 1$ and lower for $P_{21} = 0.25$ m^{-1}*

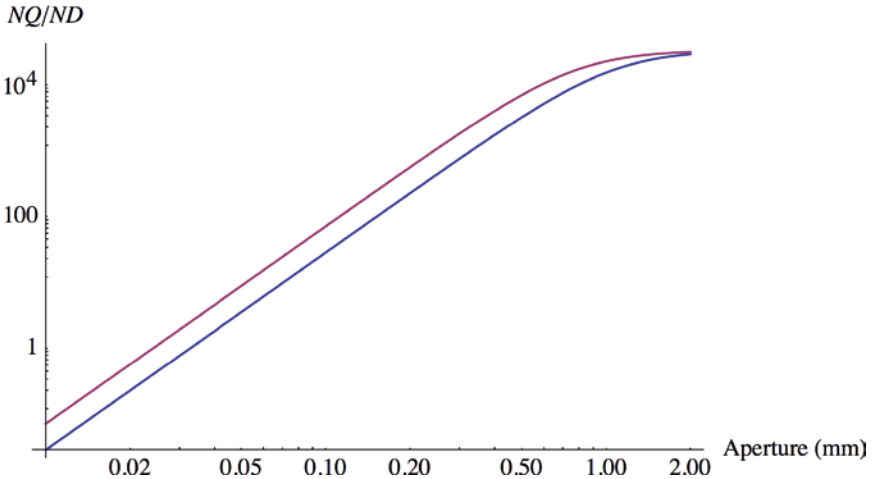

Figure 7-6. *Ratio of nuclide transport by flow to that by diffusion as function of fracture aperture. $k_T = 0.1$ and $d_p = 0.5$mm. Upper curve for $P_{21} = 1$ and lower for $P_{21} = 0.25$ m^{-1}*

8 Discussion and conclusions

The fractured walls with mm size fractures in the BMA vault would allow water to seep through the vault and carry radionuclides with it with much larger rate than the escape by molecular diffusion through intact walls. Highly permeable backfill surrounding the vault can help decrease the escape rate but it would be many orders of magnitude larger than by diffusion through intact walls. The model simulations show that the system is extremely sensitive to the fracture aperture and also quite sensitive to the size of backfill particles. There are uncertainties regarding the transmissivity of real fractures. The theoretically derived cubic law for smooth wall fracture transmissivity is known to overestimate the transmissivity of fine fracture by possibly a factor up to ten. Simulations suggest that fractures down to one or a few tenths of a mm could lead to nuclide release rates similar to those by diffusion through the intact walls of BMA. 1 mm and larger apertures may lead to many orders of magnitude larger releases even if a larger particle (50 mm) backfill is used. A smaller (5 mm) backfill will allow fractures of about 0.1 mm to transport as much nuclides as does diffusion. Very small backfill particles, 0.5 mm, will lead to very large increases in nuclide release, especially for larger fractures in the concrete walls.

It should be noted that the task as defined stipulates that the waste inside the vault has a much larger conductivity than the fractured walls and releases nuclides as if they are readily accessible. It may be worthwhile to explore if the waste could be made less permeable.

There are numerous observations that fractures self-heal due to precipitation of calcite by intruding carbonate from the air and from water. Fractures may also close by hydration of as yet un-hydrated minerals in the cement. It has not been possible to quantify the extent and rates of these processes by mechanistic modelling because of lack of suitable experimental data.

9 Notation

See also Tables 1-1, 1-2 and 1-3.

A_j	Cross section area of path j	m^2
c	Concentration	mol/m^3
c_o	Concentration at inlet to fracture	mol/m^3
C_j	Conductance of path j	m^2/s
d_p	Particle diameter	m
d_j	Thickness of barrier j	m
D_a	Apparent diffusion coefficient	m^2/s
D_e	Effective diffusion coefficient	m^2/s
D_p	Pore diffusion coefficient	m^2/s
FWS	Flow wetted surface	m^2
g	Gravitation constant	m/s^2
h	Hydraulic head	m
i	hydraulic gradient	m/m
k_T	Ratio of real to cubic law T	–
K	Hydraulic conductivity	m/s
K_d	Sorption coefficient	m^3/kg
N_D	Rate of transport by diffusion	mol/s
N_Q	Rate of transport by flow	mol/s
P_{21}	Measure of fracture frequency	1/m
Q	Flowrate	m^3/s
Q_{Low}	Flowrate below vault	m^3/s
Q_j	Flowrate in path j	m^3/s
Q_{tot}	Sum flowrate is all paths	m^3/s
Q_{Up}	Flowrate above vault	m^3/s
R_j	Resistance to flow in path j	s/m^3
R_p	Retardation factor	–
t	Time	s
t_o	Water residence time	s
t_{SS}	Time to approach steady state	s
S	Mean distance between fractures	m
T_{Cub}	Transmissivity by cubic law	m^2/s
T_{Real}	Actual transmissivity	m^2/s
T_{21}	Fracture trace length per area	m/m^2
δ	Fracture aperture	m
ε_B	Porosity of bed	–
ε_{Concr}	Porosity of concrete	–
φ_s	Shape factor	–
η_w	Viscosity of water	Pa s
ρ_{Bulk}	Mean density of the minerals in the concrete	kg/m^3
ϱ_w	Density of water	kg/m^3

References

SKB's (Svensk Kärnbränslehantering AB) publications can be found at www.skb.se/publications. References to SKB's unpublished documents are listed separately at the end of the reference list. Unpublished documents will be submitted upon request to document@skb.se.

Akhavan A, Shafaatian S-M-H, Rajabipour F, 2012. Quantifying the effects of crack width, tortuosity, and roughness on water permeability of cracked mortars. Cement and Concrete Research 42, 313–320.

Aldea C-M, Shah S P, Karr A, 1999. Permeability of cracked concrete. Materials and Structures 32, 370–376.

Bird R B, Stewart W E, Lightfoot E N, 2002. Transport phenomena. 2nd ed. New York: Wiley.

Carslaw H S, Jaeger J C, 1959. Conduction of heat in solids. 2nd ed. Oxford: Clarendon.

Coulson J M, Richardson J F, 1991. Chemical engineering. Vol 2, Particle technology and separation processes. 4th ed. Oxford: Pergamon.

Gagné R, Argouges M, 2012. A study of the natural self-healing of mortars using air-flow measurements. Materials and Structures 45, 1625–1638.

Green D W, Perry R H, 2008. Perry's chemical engineers' handbook. 8th ed. New York: Mc-Graw Hill.

Holmén J G, Stigsson M, 2001. Modelling of future hydrogeological conditions at SFR. SKB R-01-02, Svensk Kärnbränslehantering AB.

Li K, Ma M, Wang X, 2011. Experimental study of water flow behaviour in narrow fractures of cementitious materials. Cement and Concrete Composites 33, 1009–1013.

Neretnieks I, 1980. Diffusion in the rock matrix: an important factor in radionuclide retardation? Journal of Geophysical Research: Solid Earth 85, 4379–4397.

Picandet V, Khelidj A, Bellegou H, 2009. Crack effects on gas and water permeability of concretes. Cement and Concrete Research 39, 537–547.

SKB, 2014. Data report for the for the safety assessment SR-PSU. SKB TR-14-10, Svensk Kärnbränslehantering AB.

Unpublished documents

SKBdoc id, version	Title	Issuer, year
1430853 ver 1.0	Sprickor i BMA:s betongbarriär – Inspektion och orsak. (In Swedish)	Vattenfall, 2012

Appendix

Self repair

Summary of recent publications on the self repair of concrete.

De Muynck W, De Belie N, Verstraete W, 2010. Microbial carbonate precipitation in construction materials: a review. Ecological Engineering 36, 118–136.

Hearn N, 1998. Self-sealing, autogenous healing and continued hydration: what is the difference? Materials and Structures 31, 563–567.

Hearn N, Morley C T, 1997. Self-sealing property of concrete – Experimental evidence. Materials and Structures 30, 404–411.

Kan L-L, Shi H-S, 2012. Investigation of self-healing behavior of Engineered Cementitious Composites (ECC) materials. Construction and Building Materials 29, 348–356.

Lv Z, Chen H, 2012. Modeling self-healing efficiency on cracks due to unhydrated cement nuclei in cementitious materials: splitting crack mode. Science and Engineering of Composite Materials 19, 1–7.

Mihashi H, Nishiwaki T, 2012. Development of engineered self-healing and self-repairing concrete – State-of-the- art-report. Journal of Advanced Concrete Technology 10, 170–184.

Parks J, Edwards M, Vikesland P, Dudi A, 2010. Effects of bulk water chemistry on autogenous healing of concrete. Journal of Materials in Civil Engineering 22, 515–524.

Sahmaran M, Yildirim G, Erdem T K, 2013. Self-healing capability of cementitious composites incorporating different supplementary cementitious materials. Cement and Concrete Composites 35, 89–101.

Sangadji S, Schlangen E, 2012. Self-healing of concrete structures – Novel approach using porous network concrete. Journal of Advanced Concrete Technology 10, 185–194.

Van Tittelboom K, De Belie N, De Muynck W, Verstraete W, 2010. Use of bacteria to repair cracks in concrete. Cement and Concrete Research 40, 157–166.

Wiktor V, Jonkers H M, 2011. Quantification of crack-healing in novel bacteria-based self-healing concrete. Cement and Concrete Composites 33, 763–770.

Wu M, Johannesson B, Geiker M, 2012. A review: Self-healing in cementitious materials and engineered cementitious composite as a self-healing material. Construction and Building Materials 28, 571–583.

Yang Z, Hollar J, He X, Shi X, 2010. Laboratory assessment of a self-healing cementitious composite. Transportation Research Record 2142, 9–17.

Yang Y, Yang E-H, Li V C, 2011. Autogenous healing of engineered cementitious composites at early age. Cement and Concrete Research 41, 176–183.